Storage-Ring Free-Electron Laser and Chaos

Michel Billardon[a]

Laboratoire pour l'Utilisation du Rayonnement Electromagnétique,
Centre National de la Recherche Scientifique–Commissariat à l'Energie Atomique–Ministère de l'Education Nationale,
Bâtiment 209D, Université de Paris-Sud, 91405 Orsay CEDEX, France

(Received 7 February 1990)

The macrotemporal structure of a storage-ring free-electron laser is studied in relation to deterministic chaos laws. Comparison between experimental and theoretical results shows, for the first time, that the laser is determined by these laws. This can have important consequences for the future operation of free-electron lasers.

PACS numbers: 42.55.Tb, 05.45.+b, 42.60.Fc

During the last few years there has been a great deal of interest in the possibilities of free-electron lasers (FELs). The main interest of these novel coherent light sources is their tunability over a wide spectral range complemented with a high peak power. This paper deals with a particular feature of storage-ring FELs (SRFELs): the macrotemporal structure.

To recall briefly how the SRFEL operates the example of Super-ACO, the new storage ring at Orsay (France), is used. When an electron bunch circulating in the storage ring passes through a sinusoidal magnetic structure called an undulator, synchrotron radiation is emitted. The period of revolution for Super-ACO is $\theta \simeq 140$ ns and the longitudinal dimension of the electron packet is $\sigma_z \simeq 0.1$ ns. At each pass through the undulator the emitted light pulse is stored inside an optical cavity with a length such that the round-trip transit time exactly equals the electron revolution period. At each pass the electron bunch, the photon pulse, and the undulator field interact by a Compton backscattering process to give amplification and finally laser oscillation if the gain is sufficient. As a result, the SRFEL output has both a microtemporal structure of the order of a nanosecond, determined by σ_z and θ, and a macrotemporal structure of the order of microseconds to seconds, a time scale very long compared with the revolution period. This latter macrotemporal structure of the envelope of the micropulses is determined primarily by the amplification and saturation processes of the FEL. In this paper only the macrotemporal structure is discussed.

Prior to the first SRFEL experiments made on ACO, the old experiment at Orsay, it was commonly believed that the FEL would have a continuous structure. In fact, it has been experimentally established that the FEL spontaneously adopts a more or less stable pulsed structure with a repetition period of several milliseconds, as illustrated in Fig. 1. Similar results have been obtained on three different projects currently operating: ACO,[1,2] Novosibirsk,[3] and Super-ACO.[4] However, in the Super-ACO experiments cw laser operation has also been obtained, though in an unpredictable manner, the temporal structure being determined in a complicated way by the electron bunch itself in the absence of an external gain modulation. This has made it difficult for experimentalists to exactly control the characteristics of the temporal structure. In this paper we show that a stable or chaotic pulsed laser can be achieved with an external modulation, and also that the "natural" chaos seems to be due to an uncontrolled gain modulation induced by the storage ring. Here the term natural is used to designate the properties of the system resulting from the unknown and uncontrollable gain modulation induced by the storage ring, in contrast with the case of a deliberate external gain modulation.

As a first approximation, the main features of the macrotemporal structure can be described by the following model:[5]

$$\begin{aligned} \frac{dI}{dt} &= I\frac{g-p}{\theta} + i_s , \\ \frac{d(\sigma^2)}{dt} &= -\frac{2}{\tau_s}(\sigma^2-\sigma_0^2)+\alpha I , \\ g &= g_0 \exp[-k(\sigma^2-\sigma_0^2)][1+F(t)] . \end{aligned} \tag{1}$$

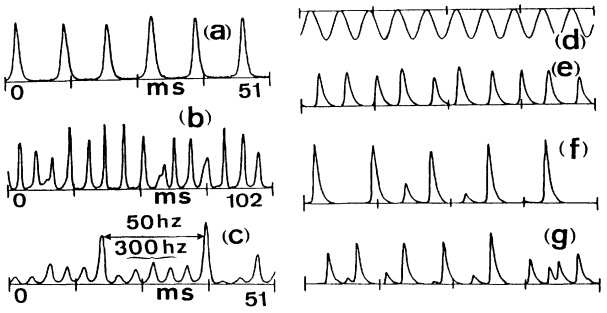

FIG. 1. Macrotemporal structure for a SRFEL operation. (a)–(c) Different results with "natural" operation obtained on ACO: (a) stable operation with a repetition rate close to resonance, (b) unstable operation, and (c) natural operation clearly synchronized by the line frequency. (e)–(g) Behavior of the Super-ACO FEL when the gain is externally modulated at 200 Hz as illustrated in (d): (e) FEL resulting from a weak gain modulation, (f) period doubling for $\Delta f/f \simeq 7\times10^{-7}$, and (g) chaotic regime when $\Delta f/f > 10^{-6}$.

The validity of this model was previously tested with the ACO experiments.[2,5] It provides good results in simulating the general FEL behavior (shape of the laser pulse, transient regimes, Q-switched operation, etc.). The first equation describes the amplification of the laser intensity I. The parameters g, p, and θ are the gain, losses, and transit time for each pass, respectively, and i_s represents the spontaneous emission from an electron bunch. The second equation describes the evolution of the electron energy dispersion $\sigma=\Delta E/E_0$, where E_0 is the average energy of electrons and ΔE the rms deviation. Without the FEL operating, the energy spread has an equilibrium value σ_0, and for a system away from equilibrium, the difference $\sigma^2-\sigma_0^2$ evolves with a characteristic damping time $\tau_s/2$. The last term, aI, represents an additional energy spread that results from the interaction between the optical field and the electron bunch. The third equation describes the evolution of the optical gain. g_0 is the maximum gain without the laser operating and the exponential term gives the gain reduction due to the effect of energy spread. The last term $F(t)$ represents an imposed modulation or fluctuation of the gain. For each variable I and $\sigma^2-\sigma_0^2$ the above equations lead to a second-order system with two very different time constants, i.e., the laser rise time $\tau_0=\theta/(g_0-p)$, several microseconds long, and the damping time τ_s, tens or hundreds of milliseconds long. The result is an oscillating system with a resonance frequency F_r and a damping time constant $\tau_s/2$. In the case of small variations around equilibrium, the resonance frequency is given by[5]

$$F_r \simeq 1/2\pi\sqrt{\tau_0\tau_s/2}. \quad (2)$$

For large variations, numerical simulations show that Eq. (2) remains approximately valid. Starting from an initial state away from equilibrium (e.g., $I=0$, $\sigma=\sigma_0$) with $F(t)=0$, this model gives a solution with damped relaxation oscillations culminating in cw laser operation as a steady-state equilibrium. Such an evolution is approximately conserved only for $F(t)$ very small, less than 1%, and explains why cw laser operation is possible on Super-ACO, a particularly stable storage ring. Normally the laser intensity temporal structure is determined by the function $F(t)$ in competition with the energy spread relaxation.

The natural pulsed structure (stable or unstable) of the first experiments has been explained with a random $F(t)$ function rather than with a periodic modulation. In fact, the simulations using our model show that a random $F(t)$ function with a wide frequency spectrum (white noise) can only result in a very unstable pulsed laser with a fluctuating intensity and a repetition rate with a wide frequency spectrum. The experimental results, as illustrated in Figs. 1(a) and 1(b), cannot be explained using only a random gain fluctuation, but a more or less stable periodic modulation in the vicinity of the resonance frequency [Eq. (2)] must be used. The important problems are (i) to know how the system responds to a periodic modulation and (ii) to elucidate the origin of the natural modulation observed in the laser.

Experiments with periodic gain modulation have been made on Super-ACO. The gain modulation is easily performed by changing the rf of the storage ring[2] which determines the electron-bunch revolution period, and therefore the overlap between the electron bunch and the stored photon pulse. A detuning $\Delta f/f \simeq 2\times10^{-6}$ is sufficient to stop the laser. However, these experiments require initially a stable cw laser, a condition rarely obtained. The response to the external modulation is sometimes augmented by additional unknown modulation, though this is normally small. Figures 1(e)–1(g) show the results of these experiments, which are also in good agreement with the theoretical simulations carried out with our simple model with $F(t)=A\sin(\Omega t)$. For a gain modulation at 200 Hz, as shown in Fig. 1(d), close to the resonance, the laser exhibits a macrotemporal structure which depends on the amplitude of the rf modulation. By varying the amplitude from 0 to $\Delta f/f=1\times10^{-6}$ (partial gain modulation), the laser first exhibits a stable modulation at the gain modulation frequency [Fig. 1(e)], then a period doubling [Fig. 1(f)], and finally chaotic evolution [Fig. 1(g)] which is roughly synchronized with the gain modulation. In fact, period doubling and chaos are easily understood because after an intense laser pulse, the gain, and therefore the delay and the structure of the next laser pulse, are determined by competition between the gain modulation and the energy spread relaxation. If both these phenomena are in accordance, then a stable pulsed laser (with or without period doubling) will occur, otherwise chaotic evolution will take place. This behavior is similar to the chaotic dynamics observed in classical lasers[6–9] and other systems. For experiments carried out at a frequency below the resonance frequency, the laser can exhibit period doubling and, more rarely, chaos, and sometimes neither. In contrast, for frequencies above the resonance frequency, period doubling or a chaotic regime is easily obtained.

For the laser operation without external modulation, as illustrated in Fig. 1, the stable limit-cycle behavior [Fig. 1(a)] and unstable [Fig. 1(b)] regimes can be compared with the modulated regimes of Figs. 1(e) and 1(g), respectively. One explanation of the natural pulsed structure is that a periodic gain modulation exists and induces a stable or unstable regime. In some cases, the modulation is clear, as in Fig. 1(c), where the laser exhibits a stable double structure at 50 Hz (the line frequency) and 300 Hz (the sixth harmonic). In this case it is clear that the gain modulation results from modulations induced by the 50-Hz main supply voltage. In contrast, for the case of Figs. 1(a) and 1(b), the quasiperiodic structure cannot be related to a perturbation with a known frequency component, except the fact that it seems close to the theoretical resonance.

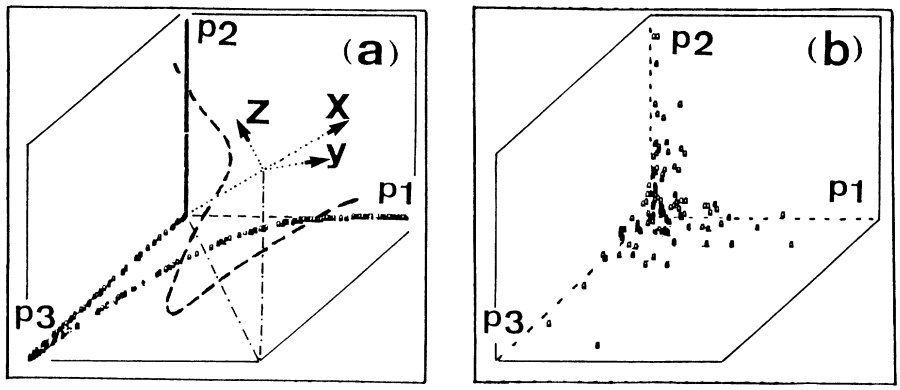

FIG. 2. An attractor represented in a 3D space; the axes P_1, P_2, and P_3 correspond to three successive laser pulses. (a) Theoretical attractors for the inverse of the laser intensity (OOO) and the half-width (---), deduced from the model with a 10% gain modulation at the resonance frequency. (b) Experimental attractor for the inverse of the laser intensity in the case of an external modulation leading to a chaotic regime as illustrated in Fig. 1(g).

The chaotic regime, as in Fig. 1(g), can be characterized by an attractor. Each laser pulse is characterized by several parameters (peak power, half-width, rise time, decay time, etc.), each having possibly different attractors. From the theoretical model one can deduce that the half-width, rise time, decay time, and inverse of the peak power are all related parameters and therefore must exhibit the same behavior. Here the common attractor is represented in a 3D space, a simplification of the total phase space. The three axes, respectively, represent the values of the chosen parameter for three successive pulses P_1, P_2, and P_3.[10] This choice of phase space is constrained by the availability of experimental data. Direct measurements of $\Delta\sigma^2$ are not possible, so that the attractor can be deduced only from laser intensity measurements. Figure 2(a) represents the theoretical attractor for the inverse of the peak power deduced from our model for a sinusoidal gain modulation at the resonance frequency with an amplitude of 10%. This attractor has a simple structure with three branches close to the axes. The attractor for the half-width is also represented and has a similar structure except that the branches are further away from the axes.

Figure 2(b) represents the experimental attractor for a chaotic laser with external modulation as in Fig. 1(g). Both attractors have roughly the same symmetry. The dispersion of the experimental attractor is probably due to residual natural modulation different from the external modulation. From this comparison it can be concluded that the chaotic regime which appears during a perfectly periodic external modulation is, probably, a deterministic chaos perturbed slowly by some imperfections of the storage ring.

Finally, we consider the experimental attractor for a natural pulsed structure as shown in Figs. 1(a) and 1(b) where we have excluded records, such as in Fig. 1(c), where a known frequency component is obvious. The resulting attractor for the rise time, the decay time, and the half-width is represented in Fig. 3, and is derived from a series of experiments conducted on ACO during several months. For convenience the attractor is presented as a projection on the Z-Y plane indicated in Fig. 2(a). The X axis is chosen as the $\langle 111 \rangle$ "symmetry" axis; i.e., three equal successive pulses give a point on this axis. It can be clearly seen in Fig. 3 that the three branches correspond to the theoretical branches P_1, P_2, and P_3 of Fig. 2(a), and represent unstable spectra as in Fig. 1(b). A set of points, denoted by S (stable), very close to the X axis, correspond to stable spectra similar to Fig. 1(a). We must note also that a theoretical attractor, determined from our model with a random $F(t)$ function, has no particular structure and is diffuse. This cannot in any way be identified with our experimental natural attractor. Therefore it is clear that the "spontaneous" attractor obeys the law of a deterministic attractor that is perturbed slowly by storage-ring imperfections. In fact, from an attentive examination of the $I(t)$ records, it appears that on a long time scale the laser has a tendency to be synchronized with the main supply voltage. The gain modulation is probably due to residual ripples of the storage-ring supplies.

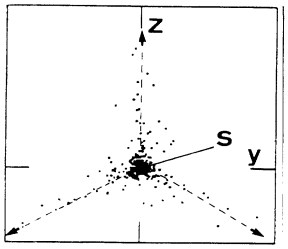

FIG. 3. Experimental attractor for the half-width, the rise time, and the decay time deduced from a series of natural operation with the ACO FEL. The axes system is indicated in Fig. 2(a). The projections of the axes P_1, P_2, and P_3 are indicated by the arrows.

To conclude, we have shown that different FEL features (period doubling, stable or chaotic macrotemporal structures, attractors, etc.), for different modulations (i.e., natural and/or external modulation), indicate that the macrotemporal structure obeys the laws of deterministic chaos. Understanding the processes that determine the natural operation is necessary to enable a perfectly stable cw laser to be obtained, i.e., in order to control the experimental components (parameters) and also to develop an efficient modulated or Q-switched FEL laser. In addition, a better understanding would be necessary to enable new Q-switch methods to also be developed. Previous Q-switched FEL experiments[3] were always performed with a large gain modulation and a very short commutation time of the order of a microsecond. Our results show that efficient Q switch is possible with a slow gain modulation, one that perturbs the electron bunch and the parameters of the storage ring much more weakly. Finally, the SRFEL can also be used to study interesting aspects of deterministic chaos.

These results were derived from several series of experiments conducted on ACO and Super-ACO, supported by Laboratoire pour l'Utilisation du Rayonnment Electromagnétique, CNRS, Commissariat à l'Energie Atomique, and Direction des Recherches, Etudes et Techniques (Contracts No. 84/080 and 85/179).

[a]Permanent address: Laboratoire Optique Physique, Ecole Supêrieure de Physique et de Chimie Industrielles, 10 rue Vauquelin, 75231 Paris CEDEX 05, France.

[1]M. Billardon, P. Elleaume, J. M. Ortega, C. Bazin, M. Bergher, M. Velghe, and Y. Petroff, Phys. Rev. Lett. **51**, 1652 (1983).

[2]M. Billardon, P. Elleaume, J. M. Ortega, C. Bazin, M. Bergher, M. Velghe, D. A. G. Deacon, and Y. Petroff, IEEE J. Quantum Electron. **21**, 805 (1985).

[3]I. B. Drobyazko, G. W. Kulipanov, V. N. Litvinenko, I. V. Pinayev, V. M. Popik, I. G. Silvestrov, A. N. Skrinsky, A. S. Sokolov, and N. A. Vinokurov, in *Free Electron Lasers II*, edited by Y. Petroff, SPIE Vol. 1133 (SPIE, Bellingham, WA, 1989), p. 2.

[4]M. E. Couprie, C. Bazin, M. Billardon, and M. Velghe, in *Free Electron Lasers II* (Ref. 3), p. 11.

[5]P. Elleaume, J. Phys. (Paris) **45**, 997 (1984).

[6]C. O. Weiss and H. King, Opt. Commun. **44**, 59 (1982).

[7]F. T. Arrechi, R. Meucci, G. Puccioni, and J. Tredicce, Phys. Rev. Lett. **49**, 1217 (1982).

[8]D. Dangoisse, P. Glorieux, and D. Hennequin, Phys. Rev. A **36**, 4775 (1987).

[9]M. J. Feigenbaum, J. Stat. Phys. **19**, 25 (1978).

[10]N. H. Packard, J. P. Crutchfield, J. D. Farmer, and R. S. Shaw, Phys. Rev. Lett. **45**, 712 (1980).